ISBN: 978-3-95450-231-8 ISSN: 2673-5490 doi: 10.18429/JACoW-IPAC2023-WEPL055

BEAM STUDY ON LOW DISPERSION CEBAF ARCS *

I. Neththikumara†[1], D. Moser[2], D. Turner[2] T. Satogata[1,2], S.A. Bogacz[2], Y. Roblin[2]
[1] Old Dominion University, 23508 Norfolk, USA
[2] Jefferson Lab, 23606 Newport News, USA

Abstract

The Continuous Electron Beam Accelerator Facility (CEBAF) at Jefferson Lab employs recirculating linac SRF technology to generate a high polarization 12 GeV electron beam for nuclear physics users. New opportunities to study multi-pass energy recovery have also emerged with the proposal of a 5-pass energy recovery demonstration, ER@CEBAF. New beam optics with minimized beta functions have been developed and tested to avoid collective beam instabilities for multi-pass beams and meet the beam requirements of the nuclear physics community. To enable energy recovery for a common arc beam transport of five passes, achromatic and isochronous arc optics conditions were satisfied by re-designing the transverse optics of CEBAF. This paper focuses on beam studies conducted to study the newly-designed, low-dispersion, lowest energy arcs for CEBAF operations and ER@CEBAF.

INTRODUCTION

The CEBAF accelerator consists with two superconducting, recirculating linacs and two vertically stacked arc segments, with 5-arcs on each of them. The accelerator has a race track shaped configuration, allowing electron beam to circulate 5.5 passes through the machine accelerating up to 12 GeV during its routine operations. Figure 1 illustrate the beam transportation layout of the CEBAF accelerator [1]. Beam delivery to the existing four halls (hall A, B, C & D) is done simultaneously, where as if required machine is capable of delivering the beam to any hall at any pass.

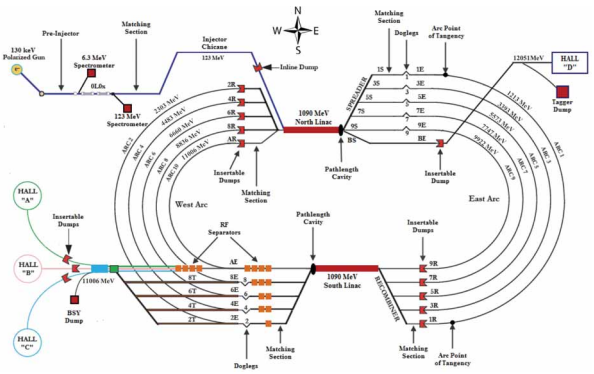

Figure 1: Layout of the CEBAF accelerator

LOW DISPERSION ARCS

In the CEBAF beamline, Arc 1 and Arc 2 are the lowest energy arcs in east and west arc segments respectively. We have redesigned the optics of these arcs to fulfill the low dispersion requirements of the proposed ER@CEBAF demo.

CEBAF linac recirculation requires the arcs to be achromatic and isochronous. Achromatic is ensured by localizing nonzero dispersion in either horizontal or vertical planes. Isochronicity is ensured by constraining the momentum compaction factor α_c, which depends on the dispersion function $D(s)$ of the lattice [2]:

$$\alpha_c \propto \int \left(\frac{D(s)}{\rho(s)}\right) ds \tag{1}$$

where $\rho(s)$ is the local bend radius, and bending between CEBAF linacs is both horizontal and vertical. Low dispersion optics were obtained by tuning the M_{56} value of the arc lattice, making the lattice to be an isochronous with α_c=0 [3].

In 2023 CEBAF optics, arcs 1 and 2 have mirror symmetric optics over the horizontal bend and peak $D_x \approx 6.0$ m to optimize synchrotron light monitor (SLM) use for momentum spread and energy diagnostics. By introducing four-fold symmetry, peak D_x is lowered to 2.5 m, but is still usable for SLM diagnostics with relocated SLMs as diagnostic $\beta_x(s)$ is similarly lowered. Improved tuning orthogonality of M_{56} and $D_x(s)$ with this low dispersion optics is an advantage for optics correction during routine CEBAF beam operations.

Jefferson Lab is also exploring the possibility of upgrading the CEBAF facility to include delivering a polarized positron beam up to 12 GeV [4]. Positrons would be generated via pair production on a tungsten target and yield a beam with relatively large energy spread and bunch length compared to present CEBAF operations, requiring lower dispersion while maintaining achromatic and isochronous recirculation in the first accelerating pass. Momentum compaction $\alpha_c = 0$ is an important requirement to avoid bunch lengthening and head-tail effects in the linac. The optics design presented here also meets the requirements for the CEBAF positron beam and 22 GeV energy upgrades.

RESULTS AND DISCUSSION

A dedicated optics study of the redesigned low dispersion CEBAF arcs was performed in early 2023. Dispersion measurement and correction, and M_{56} measurement and correction schemes defined for this specific optics, were also tested. Operating linac energy gains of 1.047 GeV were used to permit focus on arc optics tuning. Beam was transported

* This material is based upon work supported by the U.S. Department of Energy under contract DE-AC05-06OR23177.
† ineth001@odu.edu

ISBN: 978-3-95450-231-8 ISSN: 2673-5490 doi: 10.18429/JACoW-IPAC2023-WEPL055

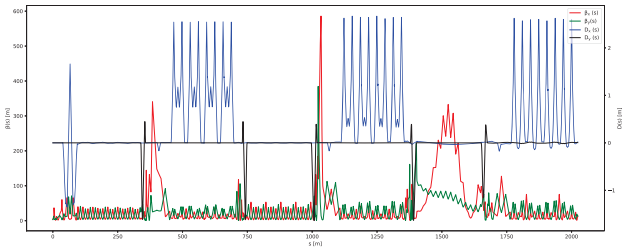

Figure 2: Optics plot of the used beamline: injector to 3R dumplet

to the 3R dumplet located in arc 3; transport optics for this study are shown in Figure 2.

Optics Initialization

Beamline settings with the matched optics of arc 1 and 2 were saved in a dedicated workspace in the CEBAF control system, and loaded into the the system using this workspace for the study. An electron beam from laser C was used in "tune" mode, with a beam current of 6 µA. The injector beam energy was ≈ 117 MeV, as required by geometric scaling from the linac energy gain per pass.

Path length corrections were performed according to the CEBAF operations procedure [5]. The dipole magnets of doglegs located at the extraction regions of arc 1 and 2 were adjusted using the *Pathlength & DogCalc12* applications for pathlength corrections.

Dispersion Measurement and Correction

Measurement of dispersion was performed by observing 30 Hz beam position monitor (BPM) orbit variation in the linacs, spreaders, arcs and recombiners, correlated with variation of a beam energy vernier. Dispersive BPM variation in the arcs up to ≈300 µm were acceptable, while larger errors required steering correction before proceeding with other optics measurements.

During CEBAF operations, dispersion measurements and correction procedures are performed by procedure [6]. For dispersion measurements, a target differential orbit of amplitude 7.5 mm on the 30 Hz BPM displays of Arc 1 at the IPM1A21 corresponds to the nominal design dispersion. For the new optics with lower dispersion, a differential orbit amplitude of 2.45 mm is required at BPM IPM1A18, two cells earlier in the arc.

The vertical dispersion of the low dispersion optics beamline is similar as of the the current optics. Hence for vertical dispersion correction, quadrupoles labeled as dispersion correctors in [5] can be used. The new low-dispersion arcs require different quadrupole knobs for correcting horizontal dispersion D_x; these quadrupole knobs are listed in Table 1 and will be incorporated into an updated operations procedure for future CEBAF runs [7].

M_{56} Measurement and Correction

Present CEBAF arc 1 and arc 2 optics have M_{56} values of 1.79 mm and 2.72 mm, respectively. The beam study involved with M_{56} measurements of these two arcs and checked the correction procedure defined for this specific optics. For the M_{56} measurements the followed procedure listed in [6]. Since the dispersion variations through both arcs are different compared to the current arc optics, a new set of correction quadrupoles are defined for M_{56} correction of arcs 1 & 2 as listed in table 2 [7].

Table 1: New D_x(s) Correction Quadrupoles

Arc	D_x(s) correction quads
Arc 1	1A35, 1A38
Arc 2	2A35, 2A38

Table 2: New M_{56} Correction Quadrupoles

Arc	Correction quadrupoles
Arc 1	1A04, 1A08, 1A14, 1A18, 1A24, 1A28, 1A34, 1A38
Arc 2	2A04, 2A08, 2A14, 2A18, 2A24, 2A28, 2A34, 2A38

Special tools designed for the machine operation system, *NL Pathlength, EnergyLocks & MyaPlot* are used in this procedure. Figure 3, illustrates the M_{56} (M56N:PEAK2) and relative momentum offset (ARC1:dpp) signal variation for Arc 1. It is observed that the M_{56} signal variation of Arc 1 does not signicantly change before and after the applied relative momentum offset. We concluded the signal variation is within the noise limit of the measurement, and gives M_{56}=0, with no required corrections.

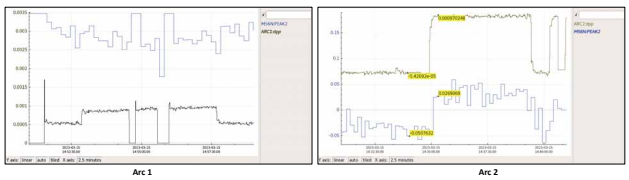

Figure 3: M_{56} signal variation corresponding to the applied momentum offset

For Arc 2, a significant variation of M_{56} signal is observed with the applied relative momentum offset (ARC2:dpp) and the calculated value using the equation 2 is 7.56 ± 7.83 cm. [6]

$$M_{56}[m] = \frac{\text{(M56N:PEAK2\_after - M56N:PEAK2\_before)}/1000}{\text{ARC2:dpp\_after - ARC2:dpp\_before}} \quad (2)$$

Using the correction quadrupoles listed in table 2, M_{56} correction is done quickly as expected. applying additional -110 G for each quadrupole.

Fast Optics Data Collection

Fast Optics (Fopt) tool is an routinely used application during CEBAF beam operations to evaluate the gross beam transport changes of the machine after Arc 1 spreader. This enables multiple beam excitation regimes, for bpm data collection. *The standard with Excitation in 1S region* is used

ISBN: 978-3-95450-231-8 ISSN: 2673-5490 doi: 10.18429/JACoW-IPAC2023-WEPL055

during the beam study for collection of data using Fopt algorithm. Four excitation dipoles (1S08H, 1E01H, 1S09H & 1E01V) are used are used to excite the beam orbit in the x/y planes and collect the BPM readings [8]. A kicker is used to excite the energy orbit, taking bpm measurements in the x/y planes. Applied kicks are of 1.48165 V. Using the collected data magnet/bpm misalignment, magnet focusing errors can be identified. The *CourantSnyder* tool is used to visualize the real time optics during a Fopt data collection.

Differential orbit measurements contain beam orbit data for an applied orbit excitation. For a Fopt data collection cycle, four separate differential orbit data files are created for respective excitation, along with additional two files for horizontal & vertical beam displacement with energy excitation.

Analysis of the collected orbit measurements is performed comparing the machine data and the orbit data of the beamline model in Elegant. Horizontal orbit kickers in the model are used to apply a kick to the beam, exciting the beam orbit 3. The required kick strength is determined by comparing the differential orbit data file for the corresponding kicker. Required orbit corrections through out the beamline is determined with the comparison or two orbits.

Table 3: Required Kick Strengths to Replicate Orbit Excitation in the Lattice Model

Kicker magnet	Kick strength [mrad]
MAZ1S08H	-3.00E-02
MAZ1E01H	-3.00E-02
MAZ1S09V	-2.70E-02
MAZ1E01V	-4.50E-02

Table 4: Required Kick Strengths for Horizontal Orbit Correction

Corrector	Kick strength [mrad]
MBT1R09H	5.00E-02
MBT2S03H	1.30E-01
MBT2S10H	-1.15E-02
MBC3S05H	-3.00E-01
MBC3S10H	1.50E-01

Orbit deviations from the model are observed in the regions with dipole magnets, especially where vertical bending of the beam occur.

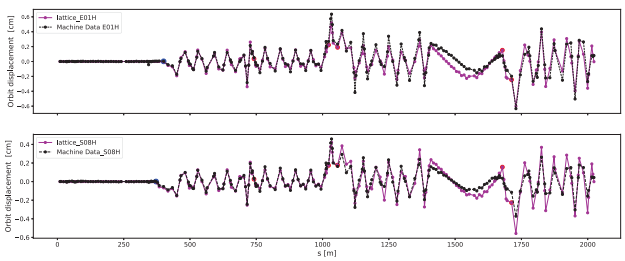

Figure 4: Matched orbits with horizontal excitation

Orbit correction for the two excited orbit is performed with adding similar corrector kicks as illustrated in figure 4. The blue circle indicate the nearest downstream BPM for the orbit excitation kicker. Since the corrector kicks are applied at the vertical bending regimes, it can be assumed that there might be errors in the model edge-focusing in dipole magnets.

Table 5: Required Kick Strengths for Vertical Orbit Correction

Corrector	Kick strength [mrad]
MBT1R07V	6.0E-02
MBT2R07V	9.0E-02
MBT2R09V	-9.0E-02
MBC3S10V	-5.0E-02
MBC3A04V	2.3E-02

A similar procedure is followed for the vertical orbit matching. Corrector kicks applied at the vertical orbit correctors are listed in table 5

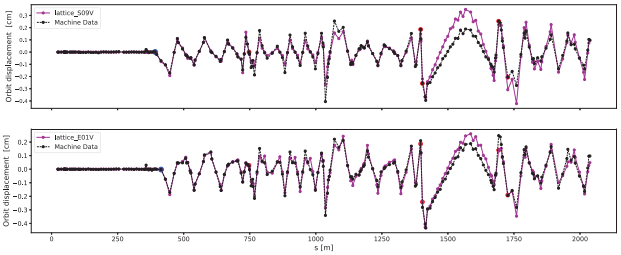

Figure 5: Matched orbits with vertical excitation

As observed in the horizontal orbit deviation, the corrector kicks applied in the model are from the regions with dipole magnets. Red circles in the plots denote the nearest downstream BPM for each orbit match corrector.

CONCLUSIONS AND FUTURE WORK

The D_x(s), and M_{56} correction scheme defined for the low dispersion arcs makes the correction procedure much easier, due to the enhanced orthogonality in low dispersion optics. Further analysis on Fopt data is useful identify magnet misalignments, focusing errors and nonlinear effects on the beamline. 6D Beam ellipse evolution studies on the same beamline is required and plan to perform RayTrace data collection & analysis for this purpose.

REFERENCES

[1] M. Spata, "Continuous Electron Beam Accelerator Facility Overview", USPAS SRF 1/29/15, https://indico.jlab.org/event/98/contributions/7445/attachments/6315/8363/18T\textunderscore-\textunderscoreCEBAF\textunderscoreUSPAS\textunderscoreSRF.pdf

[2] F. Zimmerman and M.G. Minty, *Measurement and Control of Charged Particle Beams*, New York, NY, USA: Springer, volume 1, 2003, p. 13.

ISBN: 978-3-95450-231-8 ISSN: 2673-5490 doi: 10.18429/JACoW-IPAC2023-WEPL055

[3] I. Neththikumara, S.A. Bogacz, and T. Satogata, "Re-design of CEBAF optics for ER@CEBAF", presented at the 14th Int. Particle Accelerator Conf. (IPAC'23), Venice, Italy, May 2023, paper WEPL056, this conference.

[4] J. Grames *et al.*, "Positron Beams at Ce^{+}BAF,", presented at the 14th Int. Particle Accelerator Conf. (IPAC'23), Venice, Italy, May 2023, paper MOPL152, this conference.

[5] M. Merz, "Pathlength measurement and correction procedure", CEBAF operations document MCC-PR-11-009.

[6] Y. Roblin, "Optics restoration & finalization procedure", CEBAF operations document MCC-PR-11-001.

[7] D. Turner, Y. Roblin, and T. Satogata, private communication, April 2023.

[8] "Fast Optics (Fopt) Users Guide", CEBAF operations document, Version 7.0.1.